

proportionate distribution of ash was seen in habitats dominated by either *Pinus ponderosa* or *Pseudotsuga menziesii*. The dense canopy of grand fir has also served to retard evaporation from the ash on the forest floor. As a result, the ash layer is noticeably more compacted than in either the more open *Pseudotsuga* or *Pinus* stands where the ash quickly dries after rain.

Any beneficial effect of the ashfall for the native species (for example, through release from ash-damaged competitors, reduced predation arising from the insecticide effects of the ash) is as yet unexplored in the steppe. But the white ash, where fine-textured, may have lowered soil surface temperatures and blocked physical evaporation, thus increasing the effective precipitation (10). The nutrient increment of the ash is trivial (6). Furthermore, any effect of ash in the atmosphere or precipitation probably cannot be detected because of the normal year-to-year variability in summer precipitation. The monthly totals of precipitation (in millimeters) for June, July, and August 1980 at Yakima, Lind, and Spokane, Washington, three sites along the axis of the heaviest ash fallout, were as follows: 29, trace, 7.4; 17, 1.3, 10.7; and 25, 5.3, 20, respectively (11). These values are well within 1 standard deviation of the 27-year (1951 to 1977) mean precipitation for these months for each site (12).

Ash damage to plant parts on and since 18 May is not so severe to any species as to cause extermination. Perennials such as *Balsamorhiza sagittata* and *Veratrum californicum* will certainly recover from one season of curtailed seed production. The indirect effects of the ash may prove more significant as a compacted ash layer in the arid steppe alters the distribution, frequency, and nature of seed residence sites and seed predation. The duration of this effect will depend on the rate at which the ash layer is ruptured by abiotic mechanical forces (freeze-thaw cycles, wetting-drying cycles, and erosion) and by the penetration of established perennial plants. Annuals now dependent upon germination in these ash openings may soon display diminished distribution if not prominence in these communities. Any further effects of the ash in forest and meadow steppe communities without this compacted ash layer probably will be within the amplitude exerted by more frequent climatic forces.

RICHARD N. MACK

Department of Botany,
Washington State University,
Pullman 99164

References and Notes

1. M. M. Folsom and R. R. Quinn prepared unpublished ash isopach maps for the fallout area.
2. R. Daubenmire, *Wash. Agric. Exp. Stn. Tech. Bull.* 62 (1970).
3. In contrast, Griggs' party did not reach the Katmai volcanic area in Alaska until 3 years after the cessation of activity [R. Griggs, *Ohio J. Sci.* 19, 1 (1918)], and the Tarawera eruption of 1886 in New Zealand was not studied ecologically until 1913 [B. C. Ashton, *J. Ecol.* 4, 18 (1916)].
4. C. L. Hitchcock and A. Cronquist, *Flora of the Pacific Northwest* (Univ. of Washington Press, Seattle, 1973).
5. All habitat type and zonal names follow R. Daubenmire and J. B. Daubenmire [*Wash. Agric. Exp. Stn. Tech. Bull.* 60 (1968)] and R. Daubenmire (2).
6. J. S. Fruchter *et al.*, *Science* 209, 1116 (1980).
7. I prepared as herbarium specimens the leaves of all *Balsamorhiza sagittata* individuals from 48 m² in three stands in the *Festuca-Symphoricarpos* habitat type. Sites 1, 2, and 3 received, respectively, > 20, > 15, and < 2.5 kg of ash per square meter on 18 May (1, 2). All leaf measurements were made with a digitizer [R. N. Mack and D. A. Pyke, *Ecology* 60, 459 (1979)]. Damage was defined as any obviously blackened area on a leaf. I estimated missing leaf sections by projecting the angles of leaf margins to a common distal point for these regularly deltoid leaves. A part of the leaf damage or leaf absence was due to herbivory, although this would have been minor at sites 1 and 2, where ash acted as a physical insecticide [C. A. Johansen, *Am. Bee J.* 120, 500 (1980)]. The balance of the leaf damage or leaf absence is attributable to ash in the heavy-fallout areas.
8. R. Daubenmire, *Northwest Sci.* 52, 153 (1978).
9. J. H. Brown and G. A. Lieberman, *Ecology* 54, 788 (1973); J. H. Brown, J. J. Grover, D. W. Davidson, *ibid.* 56, 987 (1975).
10. W. H. Gardner, personal communication.
11. Local climatological data, monthly summary for June, July, and August 1980 (U.S. Environmental Data and Information Service, Yakima, Wash., 1980); local climatological data, monthly summary for June, July, and August 1980 (U.S. Environmental Data and Information Service, Spokane, Wash., 1980); H. Critchfield, personal communication.
12. Local climatological data, annual summary for 1978 (U.S. Environmental Data and Information Service, Yakima, Wash., 1979); local climatological data, annual summary for 1978 (U.S. Environmental Data and Information Service, Spokane, Wash. 1979); annual summary for Washington, hourly precipitation data [No. 1-27(13), U.S. Environmental Data and Information Service, Lind, Wash., 1951-1977].
13. I gratefully acknowledge the dispatch by which support (NSF grant DEB-8020872) was provided under NSF Announcement 82 for monitoring the ephemeral changes in the biota caused by the Mount St. Helens eruption. I thank R. A. Black, H. Critchfield, E. Franz, R. Kelly, G. Long, R. Old, D. Pyke, and J. N. Thompson for help at various stages of the study.

17 March 1981; revised 22 May 1981

Mount St. Helens Eruption of 18 May 1980:

Air Waves and Explosive Yield

Abstract. *Strong atmospheric acoustic-gravity waves were recorded by sensitive microbarographs and seismographs at large distances from the Mount St. Helens eruption of 18 May 1980. Wave signatures were similar to those of waves from large nuclear explosions. Independent theoretical and empirical analyses indicate that the explosive yield of the eruption was approximately 35 megatons.*

The main eruption of Mount St. Helens on 18 May 1980 at 0830 Greenwich mean time (GMT) generated strong pressure perturbations that propagated globally and were detected by a variety of pressure-sensitive instruments. Recorded signals had characteristics typical of acoustic-gravity waves generated by large, sudden releases of energy into the atmosphere. Natural sources of such disturbances in the past have included the eruption of Krakatoa (1883) and the great Siberian meteor (1908). Artificial sources of equivalent disturbances have been large nuclear tests in the atmosphere.

The traveling waves from these large-magnitude events have two propagation modes, one controlled mainly by gravitational inertial effects and the other by the compressibility properties of the atmosphere; hence these disturbances are called acoustic-gravity waves. Characteristically, the gravity mode has a higher velocity and longer wave period (of the order of several minutes) than the acoustic mode, which has an upper limit of about 2 minutes in period at large distances. Because of the density stratification of the atmosphere, both modes show dispersion. The velocity is a func-

tion of the wave period. Such signals thus have a characteristic signature that provides ready identification.

In this study we utilized records from five special, highly sensitive microbarographs and a number of long-period vertical component seismographs that were not adequately sealed or buoyancy-compensated. Only such instruments have the proper response and sensitivity to provide data for reliable analysis of air waves.

In the microbarograph records of Fig. 1, a to e, the prominent signals are the gravity-mode (or Lamb mode) waves; the lead wave period is up to 6 minutes, and the period increases with distance as a consequence of dispersion. The dispersive character is most evident in the Hamburg and Buchholz records, which have less noise interference in this period range than most of the other records. The acoustic mode, shown by the short-period, low-amplitude waves following the main gravity wave signal, is not very prominent in any of the records. This is because the acoustic mode propagates in the channel between the stratosphere and the surface; the duct is strong when the stratospheric winds are in the direc-

Table 1. Microbarograph and seismograph data representing waves from the Mount St. Helens eruption of 18 May 1980 (origin time, 1532 GMT; location, 46.2°N, 122.2°W).

Station	Location	Range (km)	Arrival time (GMT)	Group velocity (m/sec)	Amplitude* (μbar)	Period† (sec)	Computed yield‡ (MT)
<i>Microbarograph stations</i>							
Boulder, Colorado	40.0°N, 105.2°W	1530	1655	307	460	300	39
Washington, D.C.	39.0°N, 77.1°W	3700	1850	311	210	360	33
Palisades, New York	41.4°N, 73.9°W	3950	1859.5	317	200	360	31
Hamburg, West Germany	53.5°N, 10.1°E	8000	2243	309	142	390	36.2
Buchholz, West Germany	53.4°N, 9.9°E	8010	2246.5	307	147	390	37.5
<i>Seismograph stations</i>							
Dugway, Utah	40.2°N, 112.8°W	1000	1626	309		290	
Ann Arbor, Michigan	42.3°N, 83.7°W	3056	1818	307		320	
Kings Bay, Norway	78.8°N, 11.5°E	5748	2043	308		370	
Trinidad, West Indies	10.7°N, 61.4°W	6918	2143	311		342	
De Bilt, Netherlands	52.1°N, 5.1°E	8000	2243	309		360	
Shillong, India§	25.6°N, 91.9°E	11282	0.38	302		385	

*Amplitude refers to peak-to-trough pressure change. †Period refers to the period of the first complete wave. ‡Computed yield is given in equivalent megatons (MT) of TNT; 1 MT = 4.22×10^{22} ergs (6). §Arrival time at Shillong is on 19 May; the other arrival times are on 18 May.

tion of wave propagation and weak when they are in the opposite direction.

All the stations for which records are available lie to the east of the source. In May the stratospheric winds are easterly (blow from the east) and opposite to the direction of propagation; hence the acoustic mode is weak. To illustrate this effect, note the signal from two nuclear

explosions (Fig. 1, f and g) recorded at our station in Berkeley, California, from tests in the American Pacific test range and in Novaya Zemlya, respectively. The strong acoustic mode in Fig. 1f from a source to the west was recorded when the stratospheric winds were westerly (as they are in winter) or favorable. The weak acoustic mode in Fig. 1g was re-

corded from a source to the east, with the stratospheric westerly winds opposite to the direction of propagation. The record in Fig. 1g more closely resembles those from Mount St. Helens.

On the basis of the distance to the eruption source and the wave travel time (arrival time minus origin time), the wave group velocities to each recording

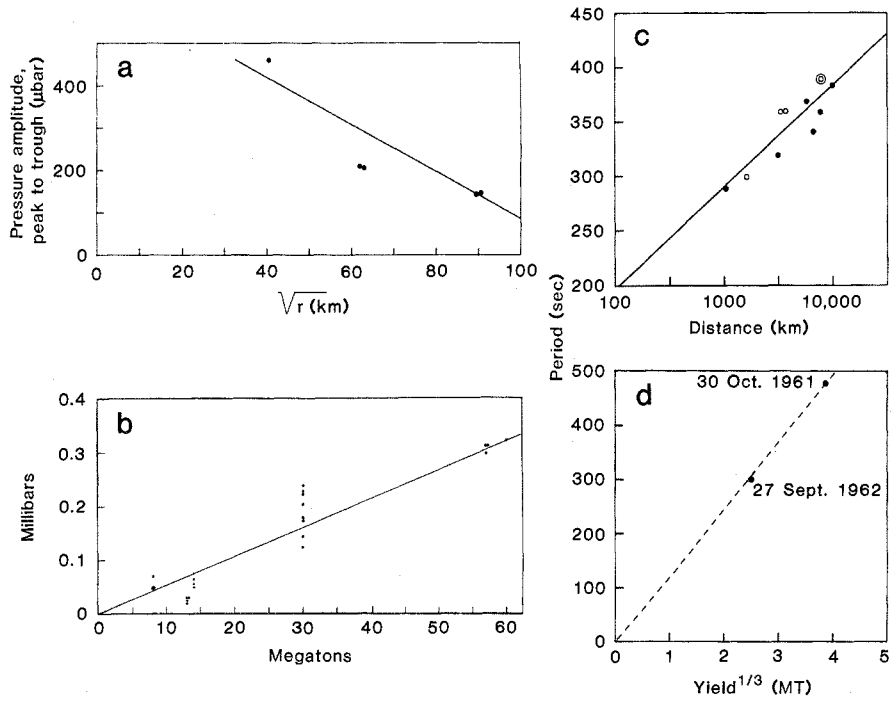
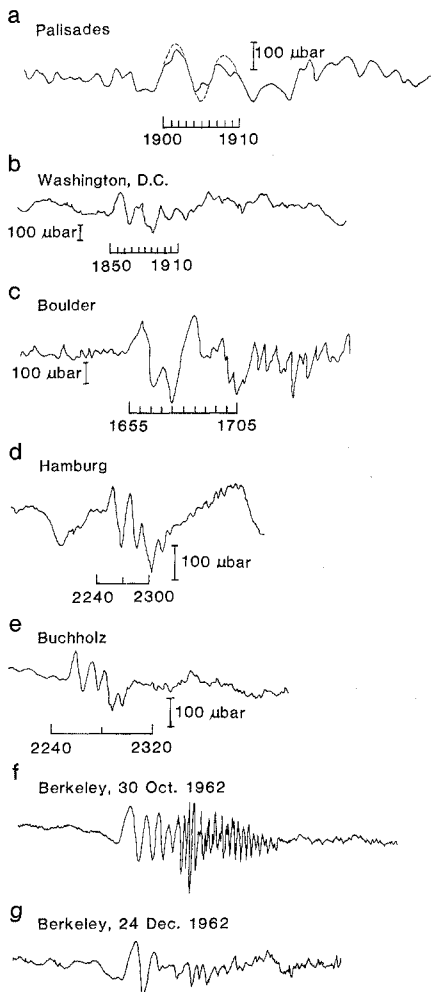


Fig. 1 (left). (a to e) Air waves from the Mount St. Helens explosive eruption for the stations described in Table 1. Time shown is Greenwich mean time. Data sources are acknowledged in (7). (f and g) Traces from nuclear explosions. Fig. 2 (right). (a) Pressure amplitude versus square root of distance for the Mount St. Helens eruption. (b) Amplitude versus yield for pressure waves from nuclear explosions in Novaya Zemlya (range, 6600 km) recorded by an array of four instruments around Palisades (4). (c) Period versus distance for the lead air waves in (○) microbarograph and (●) seismograph traces following the Mount St. Helens eruption. (d) Period versus cube root of yield for tests in Novaya Zemlya recorded by the array around Palisades.

site were calculated. These values, which range from 302 to 317 m/sec, are similar to scores of values determined for acoustic-gravity waves generated by nuclear explosions at different test sites and detected at globally distributed recorders (1). They also match the theoretical computations for such propagation (2). On the basis of signal appearance and appropriate group velocities (or arrival times), we concluded that signals shown in Fig. 1, a to e, were generated by the eruption of Mount St. Helens.

From pressure amplitudes and periods it is possible to compute the probable explosive energy or yield of the eruption, but not the total energy of the entire event. We used separate theoretical and empirical procedures for this purpose.

1) Posey and Pierce (3) developed the following approximate theoretical relationship among energy, pressure perturbation amplitude, and period for an explosion in the atmosphere:

$$E = 13 P[R \sin(r/R)]^{1/2} H_s (cT)^{3/2}$$

where E is energy (ergs), P is the first peak-to-trough pressure change (microbars), R is the radius of the earth (centimeters), r is the great circle distance from source to receiver, H_s is the scale height of the atmosphere (taken as 8 km), c is the speed of sound, and T is the wave period (seconds) for the first full wave. From the microbarograph data in Table 1 we computed the yields in megatons (MT) shown in the last column. The average yield is 35 MT.

2) Figure 2a is a plot of pressure amplitude against distance, where the square root of the latter is used because the cylindrical spreading of the gravity waves causes amplitude to decrease as $1/\sqrt{r}$. A straight line has been fitted to the points. Figure 2b is an earlier graph (4) of pressure against yield for a number of tests in Novaya Zemlya that were recorded by several instruments in our array of four stations around Palisades, New York. Using the distance from Novaya Zemlya to Palisades (6600 km) in Fig. 2a, we obtain the pressure amplitude for Mount St. Helens for that distance. The resulting value of 190 μ bar corresponds to a yield of 35 MT in Fig. 2b, which matches the theoretical calculation above.

3) In another empirical analysis, we used wave period as a tool to estimate yield. In addition to the periods from microbarographs in Table 1, we used values from long-period vertical seismographs at widely distributed locations. Seismic drum records have much higher time resolution than most microbarographs, so that period measurements

with good accuracy are obtainable [see, for example, the record from De Bilt in the Netherlands (5)]. The data from the seismographs are also given in Table 1. Like the microbarograph signals, the seismograph data yield normal group velocities between source and receivers. Figure 2c shows the period of the first full wave plotted against distance and indicates the dispersion effect described earlier. Only records from stations at least 1000 km from Mount St. Helens were used, to ensure that the lead gravity wave was fully established. Figure 2d shows the period plotted against cube root of yield, where the periods are based on waves from tests at Novaya Zemlya that were recorded on the Palisades array. It is known that wave period varies as the cube root of yield. Only two points in which we have confidence in the yield are plotted, together with zero. Using 6600 km for the distance from Novaya Zemlya, we obtain an equivalent period of 365 seconds from Fig. 2c. This equivalent period corresponds to a yield of 30 MT (from Fig. 2d) for the Mount St. Helens explosion, in good agreement with the theoretical and empirical estimates given above.

On the basis of the best available evidence, we conclude that the explosive yield of the main Mount St. Helens eruption

on 18 May 1980 at 1532 GMT was roughly 35 MT (1.48×10^{24} ergs).

Note added in proof: Records from Hawaii and Japan, the only stations with records available to the west of the source, indicate a somewhat lower yield (about 25 MT).

WILLIAM L. DONN
NAMBATH K. BALACHANDRAN
*Lamont-Doherty Geological
Observatory of Columbia University,
Palisades, New York 10964*

References and Notes

1. W. Donn and D. Shaw, *Rev. Geophys.* **5**, 53 (1967).
2. N. K. Balachandran, *J. Acoust. Soc. Am.* **48** (Part 2) 211 (1970).
3. J. Posey and A. Pierce, *Nature (London)* **232**, 253 (1971).
4. W. Donn, D. Shaw, A. Hubbard, *IEEE Trans. Nucl. Sci.* **NS-10**, 285 (1963).
5. A. R. Ritsema, *Eos* **61**, 1202 (1980).
6. S. Glasstone and P. Dolan, *The Effects of Nuclear Weapons* (Department of Defense and Department of Energy, Washington, D.C., 1977), p. 43.
7. We are grateful to G. Stilke (University of Hamburg), A. R. Ritsema (Royal Netherlands Meteorological Institute), and W. Hoecker and A. Bedard (National Oceanic and Atmospheric Administration) who provided copies of records from their instruments and to J. Jordan and R. Hunter (USGS Seismology Branch, Denver) for seismograms from the Global Seismic System. This work was supported by grant ATM-08350 from the National Science Foundation, grant NAS 8-33378 from the National Aeronautics and Space Administration, and grant DAAG 0131 from the U.S. Army Research Office. This is Lamont-Doherty Geological Observatory Contribution 3187.

26 January 1981; revised 17 April 1981

Rapid Massive Assembly of Tight Junction Strands

Abstract. *Incubation at 37°C of excised rat prostate tissue results in massive proliferative assembly of new tight junction strands along the entire length of the lateral plasma membranes of the columnar epithelial cells. The new tight junction elements are assembled within 5 minutes and have an average length six times that of those present in the apical tight junction band. Massive assembly occurs in the presence of protein synthesis inhibitors (cycloheximide) or of metabolic uncouplers (dinitrophenol). Thus, proliferative assembly of tight junction strands involves molecular reorganization from a pool of preexisting, probably membrane-associated, components. The fascia occludens and some examples of experimentally induced tight junction proliferation may reflect the massive emergence of tight junction strands when tissue is subjected to diverse stressful conditions.*

The tight junction (occluding junction, zonula occludens) is a specialized intercellular contact between adjacent epithelial cells that assures the physical separation of luminal and intercellular spaces. Current views of tight junction structure derive from the morphological analysis of thin section (1) and freeze-fracture (2) preparations as seen by electron microscopy. In these studies, the tight junction is described as a network of anastomosing strands visible on the protoplasmic fracture face (3), with corresponding furrows observed on the exoplasmic face. As in many other epithelial cells, the strands are predominantly oriented par-

allel to the edge that separates luminal from lateral regions of the plasma membrane. They generally number less than 15 and may also exist in other regions of the plasma membrane, for example, in places where the polarity of the cells is less marked.

The chemical nature and the supramolecular organization of the tight junction components are virtually unknown, and their biogenesis and assembly are poorly understood. Evidence from freeze-fracture studies indicates that a single or double filament may be the main structural element of this junction (2). Studies of its mode of assembly have been hin-